ACS Photonics

pubs.acs.org/journal/apchd5

Article

Facile Measurement of the Rotation of a Single Optically Trapped Nanoparticle Using the Diagonal Ratio of a Quadrant Photodiode

Yuval Yifat, John Parker, Tian-Song Deng, Stephen K. Gray, Stuart A. Rice, and Norbert F. Scherer*

Cite This: *ACS Photonics* 2021, 8, 3162–3172

Read Online

ACCESS | Metrics & More | Article Recommendations | Supporting Information

ABSTRACT: Optical tweezers are a powerful tool for exploring physical properties of particles in various environments through analysis of their dynamics in a trapping potential. Analysis of the trapped particle's position is often done using interferometric back-focal-plane detection microscopy in which interference between the trapping laser and the light interacting with the trapped particle is projected on a quadrant photo-diode (QPD). The QPD measurements are almost universally the voltage ratios between the *transverse components* of the detector (left/right; up/down) that are calibrated to ascertain particle positions and orientations (*i.e.*, rotation). In this paper, we demonstrate how measuring the *diagonal ratio* of the QPD allows tracking the spinning and orbital motion of optically trapped objects with enhanced sensitivity compared to the conventional transverse ratio and reveals additional information about particle dynamics. The diagonal ratio "balances" the signal from opposite sides of the QPD, allowing common mode noise reduction and increased measurement sensitivity of the rotating nanospheres at frequencies from below 200 Hz to above 15 kHz. We show that the variability in particle rotation rates is due to slight differences in the aspect ratio of the nanoparticles. We also measure *in situ* a gradual acceleration in the spinning frequency of trapped nanoparticles due to photothermal shedding of surface ligands and the resulting decrease of rotational friction in solution. The accelerating particles spin at rates exceeding 30 kHz and are eventually "optically printed" onto the glass coverslip on top of the liquid cell enclosure. The diagonal ratio is a simple, readily available, and powerful enabler for measuring rotational dynamics with a 5-fold sensitivity increase over conventional QPD measurements. This affords opportunities for controlling the orientational dynamics of trapped nanoparticles, which is crucial for various applications, including nanoscale mechanical motors.

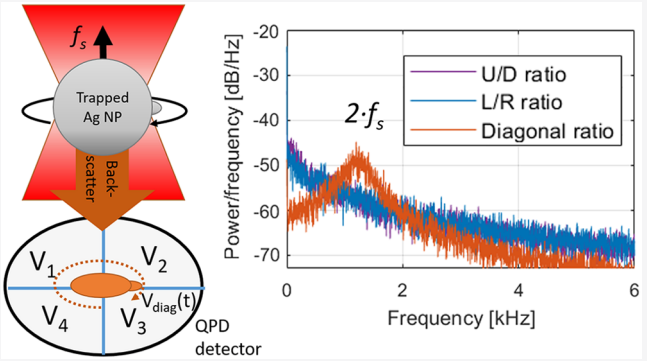

KEYWORDS: *optical tweezers, optical trapping, optical sensing, quadrant photodiode, nanoparticle rotation, angular momentum*

INTRODUCTION

The development of new experimental methods are often motivated by a desire to better understand the manner in which systems interact with their environment and also the desire to control that interaction or gain control over natural forces. For example, there are several measurement and analysis methods for determining the rotational speed of a microscopic object of interest. A simple and commonly used method is image analysis of a captured video of a trapped object.[1−3] This requires that the trapped object be imaged at high frame rates, and the resulting video undergoes image processing and analysis to ascertain the particle orientation. However, this method requires that the object be visibly asymmetric (i.e., discernible beyond the diffraction limit) so that its rotation can be tracked and that the object's rotation rate be slower than the camera frame rate. Alternatively, collecting the scattered light from the nanoparticle and analyzing its autocorrelation signal[4,5] or power spectral density[6] allows high-speed tracking of trapped nanoparticle rotation, but the information obtained in this method is limited because it uses only a single detector. A "torque detector" measures the ratio between the scattered left-handed and right-handed circularly polarized (CP) light.[7,8] However, this method is applicable only when the laser beam driving the rotation is linearly polarized (LP), and the torque is obtained by changing the LP direction in a periodic fashion. Thus, this method would not work for cases where a trapped particle is driven by CP light. An additional measurement technique is splitting the light between two parts of a balanced photodiode,[9,10] which requires delicate calibration of the optical beam and multiple detectors to identify particle position and

Received: May 31, 2021
Published: November 2, 2021

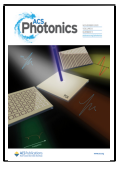

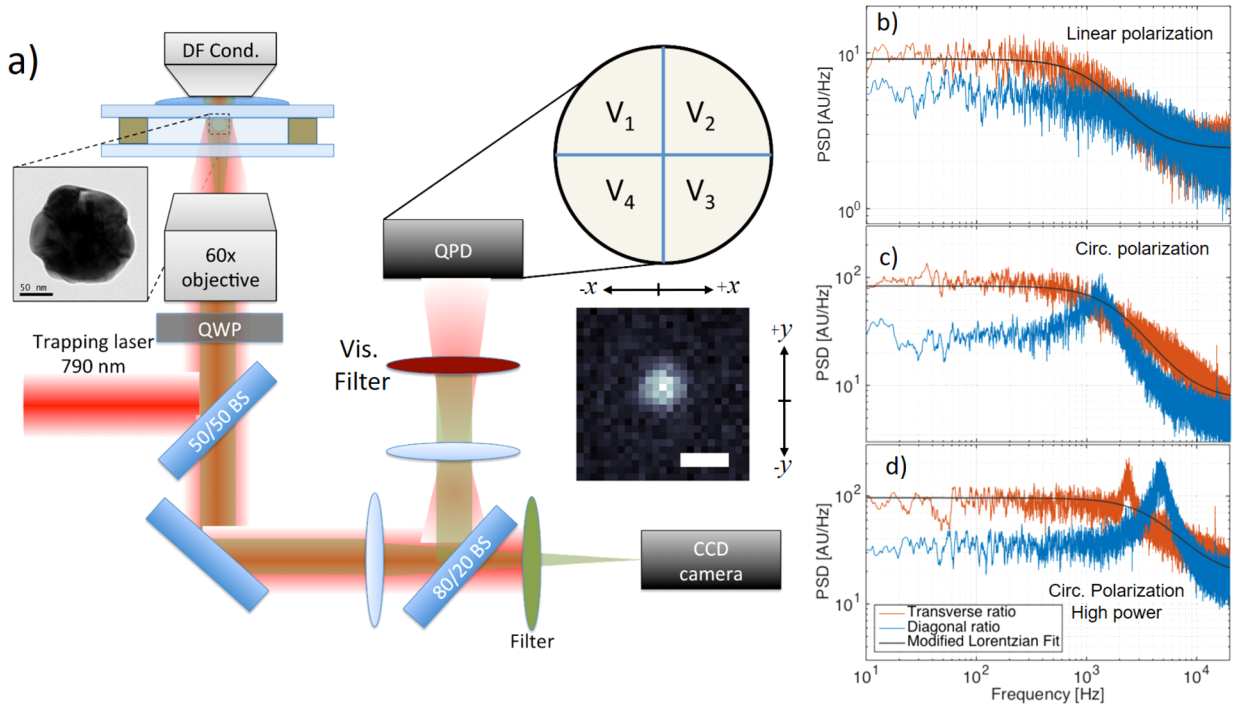

Figure 1. Experimental setup and experimental QPD power spectral density results. (a) Experimental optical trapping setup. DF Cond, darkfield condenser; QWP, quarter waveplate; BS, beam splitter; QPD, quadrant photodiode. Left inset: TEM image of a representative 150 nm Ag nanoparticle taken at a magnification of 75 000×. Note that the particle is slightly aspherical. Scale bar is 50 nm. Right inset: representative image of a single 150 nm Ag nanoparticle in a Gaussian trap (200 μs acquisition time). Scale bar is 350 nm. (b) Normalized power spectral density of the transverse (U/D ratio; red) and the diagonal (blue) ratios of the QPD when a single particle is trapped in a linearly polarized Gaussian trap with an incident intensity of P_{in} = 9 mW. The black line is a fit of a Lorentzian function, which is typically used to calculate the stiffness of the trap from the transverse ratio.[28] Note that the PSD noise level of the diagonal ratio is lower than that of the transverse ratio. (c) Normalized PSD values of the same particle in a circularly polarized trap (P_{in} = 9 mW). Note the emergence of a peak in the diagonal ratio at a frequency of ∼1.3 kHz. (d) Normalized PSD values of a particle trapped in a circularly polarized Gaussian trap with high incident power (P_{in} = 17 mW). We observe a peak in the diagonal ratio at a frequency of ∼4.7 kHz and a peak in the transverse ratio with a frequency of ∼2.35 kHz (one-half the frequency of the diagonal ratio). The peaks correspond to a particle rotational frequency of ∼2.35 kHz (see text).

orientation. Arguably, the most common approach to measuring the rotational motion of a nanoparticle is from the power spectral density (PSD) of position-sensitive detectors, including quadrant photodiodes.[6,11]

Since Ashkin and co-workers first reported[12] the manipulation of micrometer-scale particles using laser radiation, optical tweezers have become an important research tool in the study of micro- and nanoscale objects.[13,14] Optical tweezers enable sensitive *in situ* measurements of the forces acting on nanoscale objects such as biological molecules and motors[15] or nanoparticles.[16,17] The broad applicability arises, in no small measure, from the accurate measurement of the position of an object in a harmonic optical trap potential using high-speed position-sensitive detectors as first demonstrated by Gittes *et al.*[18] These nonimaging measurements allow position detection via the interference between the trapping beam and the light (forward) scattered from a particle trapped in the beam. Essential attributes and asymmetries of this interference pattern projected onto the back focal plane of the microscope are rapidly measured using a quadrant photodiode (QPD) or a position sensitive detector. The detector readout is used to establish the particle position.[18−21] QPDs are ubiquitous in optical tweezer experiments as they allow determining the trap stiffness and particle position by measuring the voltage ratios between *transverse sectors* (i.e., left/right and up/down). Examples of particle positioning using QPDs have been reported in both forward[19] and backscattered directions.[22]

These optical tweezer measurement systems have been fundamentally important tools for understanding the dynamics and underlying nanomechanical forces in both biological and condensed matter systems, including the accurate and precise measurement of the linear[23,24] and torsional[25] spring constants of DNA and the binding forces of proteins.[26−28] Similar measurements have been applied to nano- and microcolloidal systems to understand the fundamental nature of Brownian motion,[29] to trap and align anisotropic nanoparticles,[30−32] and to rapidly rotate nanoscale objects such as nanospheres[3,4] or nanorods.[32,33] The latter asymmetrical objects were shown to rotate at frequencies in excess of 10 kHz, enhancing the realization of optically controlled nanomotors.[34,35]

However, while the QPD transverse ratios are exquisitely sensitive for displacements, measurement of rotation (i.e., spinning) requires significant anisotropy or asperities of the trapped (nano-) particles and rotation of the particles at high rotation rates in order to get sufficiently high SNRs (*e.g.*, previous reports of rotation of trapped spherical nanoparticles discuss rotation frequencies higher than 1 kHz[4,35]). Greater sensitivity to rotational motion at low frequencies would allow trapping of particles at lower optical powers, reducing detrimental effects to the particles (*e.g.*, heating,[36] sticking nanoparticles on the surface,[37] or photothermal degradation of surface ligands[38]). In addition, slower, more controlled rotational measurement is necessary for more accurate

https://doi.org/10.1021/acsphotonics.1c00802
ACS Photonics 2021, 8, 3162−3172

nanomotors[39] and more sensitive measurement of biological phenomena.[28]

In this paper, we demonstrate measurements of the rotational and orbital motion of single trapped spherical Ag and ultraspherical Au nanoparticles using measurements of the *diagonal ratio* of a QPD demonstrating 5-fold greater sensitivity to spinning motion versus the traditional transverse ratio type measurement. The use of the diagonal ratio of the QPD has been suggested in the past[40] for asymmetric mesoscale rods at low frequencies (of several Hz). In this paper we expand the use of the diagonal ratio by applying it to nanoparticles at a large range of frequencies (up to 30 kHz), limited only by the sampling rate of the QPD and accompanying electronics. We also expand the theoretical framework for understanding the use of the diagonal ratio by modeling the QPD signals with analytical descriptions of the fields scattered from model (idealized) spherical nanoparticles with defined asperities and discuss the difference between spinning motion and orbital rotation of the particle in the optical trap. In addition, we model the QPD signals assuming different explicit motions (*e.g.*, spinning, orbiting, and Brownian motion) and perform electrodynamics–Langevin dynamics simulations of single nanoparticles to model realistic motion with knowledge of ground truth properties. Using the QPD diagonal ratio allows tracking highly symmetrical objects (as opposed to video tracking), allows measurement at low (<200 Hz) spinning frequencies (as opposed to autocorrelation methods), and is very easy to align and operate in a standard optical trapping setup (compared to torque-meters or balanced photodiodes).

EXPERIMENTAL SECTION

Our experimental setup, shown in Figure 1a, consists of a trapping laser beam (CW Ti:sapphire; Spectra-Physics 3900S) operating at a wavelength of 790 nm, which is reflected off a 50/50 beam splitter, passes through a quarter waveplate to control the beam polarization, and is focused with a 60× water immersion objective (Nikon 60× Plan APO IR, NA = 1.27) into a sample cell. The samples we study are a 1:200 dispersion of Ag (or Au) nanoparticles in DI water. The particles have a diameter of either 150 nm (NanoComposix, NanoXact Silver KJW1882 0.02 mg/mL; see left inset of Figure 1a for a representative TEM image of Ag nanoparticle) or 200 nm (NanoComposix, NanoXact Silver DAC1326 0.02 mg/mL) or "ultra-spherical" Au nanoparticles (see the Supporting Information). The beam is focused slightly beneath the top coverslip (beam propagating upward in the lab frame) and has a measured fwhm of 500 nm at the focal plane.

The particles are also illuminated by incoherent visible light using a darkfield condenser positioned above the coverslip sandwich containing the nanoparticle solution. The light backscattered from the particles is transmitted through the microscope objective and optical system and a 1.5× optical expander to a sCMOS camera (Andor Neo; 6.5um sq. pixels), which is used to image the particles. A representative frame (image) from the camera is shown in the right inset in Figure 1a. The magnification of the optical system gives an effective pixel size of 72 nm/pixel. In addition to the imaging system, our setup was designed to allow measurement of the interference signal between the light scattered from the particles and the reflected beam from the water–coverslip interface in a backscattered geometry (see Carter *et al.*[22] for an example of a similar setup). This approach allows back-focal plane measurement along with darkfield microscopy, thereby enabling imaging of subdiffraction limit particles such as Ag nanoparticles. More importantly, because the reflection from the coverslip is small (Fresnel reflection from the glass–water interface is calculated to be 0.4% of the incident intensity at normal incidence), backscattered detection allows for accurate, high signal-to-background ratio measurements of the particle position without operating the QPD near saturation with the large noise inherent to the incident laser light.[41]

The transverse ratio signals (up/down and left/right) are defined from the four (time series of) measured voltages from the QPD $V_i(t)$, $i = 1-4$ (orientation of the QPD is shown in Figure 1a), as

$$U/D = \frac{(V_1 + V_2) - (V_3 + V_4)}{\sum_i V_i} \tag{1a}$$

$$L/R = \frac{(V_1 + V_4) - (V_2 + V_3)}{\sum_i V_i} \tag{1b}$$

It has been demonstrated that for small particles (considered as Rayleigh scatterers) and for small displacements relative to the Gaussian beam diameter[19,28,41,42] the transverse ratios in eqs 1a and 1b are proportional to the x and y particle displacements in the focal plane. We similarly define the diagonal ratio to be

$$\text{Diag.} = \frac{(V_1 + V_3) - (V_2 + V_4)}{\sum_i V_i} \tag{2}$$

Here, an imbalance in the voltages corresponds to an angular asymmetry in the light collected by the detector. We will show that this ratio is sensitive to rotational motion of nanoparticles that are minutely asymmetric.

Figure 1b–d demonstrates the enhanced sensitivity inherent to the diagonal ratio signal. We trapped a single 150 nm diameter Ag nanoparticle in a linearly polarized (LP) focused trap with an incident power of P_{in} = 9 mW and measured the four voltages from the QPD at a sampling rate of 62.5 kHz using an analog-to-digital converter (A2D; National Instruments NI USB-6210). A power spectral density (PSD) plot of the results for the U/D ratio and diagonal ratios is shown in Figure 1b (note that the L/R ratio gives the same signal and results as the U/D ratio). We fit the transverse ratio with a Lorentzian function that is indicated with a black curve (the corner frequency of the fitted curve is f_c = 1.5 kHz).

We repeated the experiment with CP light at an incident intensity of P_{in} = 9 mW (Figure 1c) and observed the emergence of a peak in the diagonal ratio with a frequency of 1.3 kHz. The transverse ratio remained similar to the case in which the particle is trapped in LP light; that is, no peak is evident. When the incident power is increased to P_{in} = 17 mW (Figure 1d), the peak in the diagonal ratio increases to 4.7 kHz. We also note the emergence of a peak in the transverse ratios with a frequency of 2.35 kHz, one-half of that observed in the diagonal ratio. These results suggest that the diagonal ratio allows measurement of rotational signals at significantly lower incident optical powers (and therefore lower spinning frequencies) than the transverse ratios.

SIMULATION OF QPD VOLTAGES COMPARING TRANSVERSE AND DIAGONAL RATIOS

The peaks observed in the PSDs shown in Figure 1b,c and the relationship between the transverse and the diagonal

https://doi.org/10.1021/acsphotonics.1c00802
ACS Photonics 2021, 8, 3162–3172

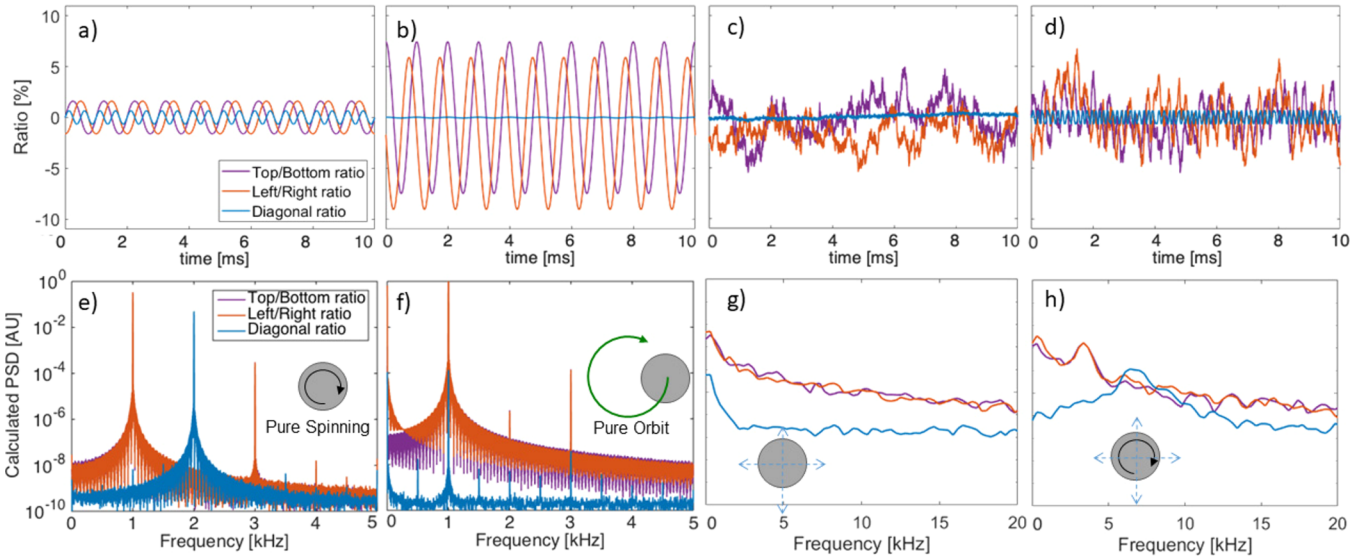

Figure 2. Simulated QPD voltages, voltage ratios, and power spectra for a single 150 nm Ag nanoparticle undergoing different types of motion. (a–d) Time series of transverse ratios (purple and red) and the diagonal ratio (blue) of the QPD when a single particle is undergoing (a) pure spinning motion around its axis at the center of the Gaussian trap (spinning frequency is 1 kHz); (b) pure orbit of the particle about the center of the Gaussian trap. Orbital radius is 150 nm; orbital frequency is 1 kHz. (c) Confined motion of the particle in the center of an LP Gaussian trap with white noise forces acting on the particle (random fluctuations were chosen to mimic Brownian motion). (d) Confined motion of the particle in the center of a CP Gaussian trap with white noise. (e–h) Normalized power spectral densities (PSDs) of the particle undergoing the motion described in panels a–d, respectively. Panels c, d, g, and h use the same color scheme as panels a, b, e, and f.

components can be understood by simulating the scattered intensity from a trapped particle undergoing different types of motion (see Figure 2). Using the notation introduced by Gittes *et al.*,[18] a focused Gaussian beam with intensity I_{tot}, waist diameter w_0, and wavelength λ_0, is focused at the position $r = 0$. The outgoing unscattered electric field that is back-reflected from the coverslip is

$$E(\mathbf{r}) \approx R\frac{-ikw_0 I_{tot}^{1/2}}{r(\pi\epsilon_s c_s)^{1/2}}\exp\left[ikr - \frac{k^2 w_0^2\theta^2}{4} + i\pi\right] \quad (3)$$

where R is the Fresnel reflection ratio of the field (0.6% for normal incidence between water and glass); $k = \frac{2\pi n_s}{\lambda_0}$ is the wavenumber of the incident field; ϵ_s, n_s, and c_s are the permittivity, refractive index, and speed of light in the water medium, respectively. The additional factor of $i\pi$ in the exponent is due to the reflection from the coverslip. $-\frac{\pi}{2} \le \theta \le \frac{\pi}{2}$ is the inclination angle of the field relative to the propagation axis of the incident field (defined as the $+z$ direction). We place a particle at the focal plane at a position (x_0, y_0) away from the center of the optical trap (*i.e.*, trap centered at (0,0)). The unscattered field at the particle location (x_0, y_0) is

$$E(x, y) = \frac{2I_{tot}^{1/2}}{w_0(\pi\epsilon_{sc_s})^{1/2}}e^{-(x_0^2+y_0^2)/w_0^2} \quad (4)$$

For a particle with polarizability α, the Rayleigh approximation of the scattered field at large r is

$$E_{scat}(\mathbf{r}) \approx \frac{k^2\alpha}{r}E(x_0, y_0)\exp\{ik\cdot[(r - x\sin(\theta)\cos(\phi))\cdot(r - y\sin(\theta)\sin(\phi))]\}\cdot g(\theta, \phi) \quad (5)$$

Finally $g(\theta, \phi)$

$$g(\theta, \phi) = 1 + A\cdot e^{-(\theta-\theta_0)^2/2\sigma_\theta^2}e^{-(\phi-\phi_0)^2/2\sigma_\phi^2} \quad (6)$$

is a geometric function we introduced to model the aspherical nature of the trapped particles (see inset in Figure 1a and the Supporting Information); θ_0 and ϕ_0 are the angles to which the perturbed field is projected; $\sigma_{\theta,\phi}$ are the fwhm angular widths of the excess field projection. Asymmetric particles will scatter light in a nonuniform fashion, and our model assumes a slight perturbation to the field that increases the scattering in a specified solid angle. Here A is the magnitude of the geometric effect (taken in our simulation as 0.05; if $A = 0$ there is no perturbation).

Using the calculated unscattered field (eq 3) and scattered field (eq 5) one can calculate the total field at the back-focal plane and the intensity, which includes the interference between the fields. Thus, given a trajectory of the position $x(t)$, $y(t)$, and orientation $\phi(t)$ of a trapped particle, we can calculate the resulting projected intensity in the back-reflected back-focal plane and integrate the resulting field within each of the four quadrants of the QPD, giving normalized ratios of $V_i/\sum V_i$, $i = 1, ..., 4$. The voltage ratios are used to calculate the voltage time trajectories and their associated PSDs.

Figure 2a,e shows the calculated transverse and diagonal QPD ratios as well as the PSD for a particle located at the center of the Gaussian trap and spinning around the z axis (*i.e.*, around an axis of rotation along the beam propagation direction) at a frequency of $f_s = 1$ kHz. The result of this motion is a peak in the transverse ratio at f_s (red curve for the L/R ratio; the purple curve representing the U/D ratio is identical) and a peak in the diagonal ratio of $2f_s$ (blue curve). The baseline noise level in these simulations was set by limiting the calculated values to a 16-bit range (equivalent to our experimental sampling depth). *The reason for the doubling of the sampled frequency between the transverse and the diagonal ratios*

https://doi.org/10.1021/acsphotonics.1c00802
ACS Photonics 2021, 8, 3162–3172

is that the diagonal signal is twofold symmetric; that is, an increase in the voltage V_1 due to enhanced scattering on that quadrant will give the same diagonal ratio as an increase in the voltage V_3. As a result, a complete rotation of the asymmetric particle around its axis will give two maxima in the diagonal ratio signal: once when the particle is oriented at 45° and once when it is oriented at 225° (*i.e.*, as $\sin(2\theta)$ as opposed to $\sin(\theta)$). This frequency doubling is evident in the time trajectories in Figure 2a: the blue curve representing the diagonal ratio is a sinusoidal function with twice the frequency of the red and purple curves that represent the transverse ratios. The doubled frequency of the diagonal ratio versus the transverse ratio signal is evident in the experimental results in Figure 1c,d. Note that the amplitude of the peak in the PSD associated with the spinning frequency depends on the aspherical nature of the particle as presented in eq 5. If a perfectly spherical particle were spinning at the center of the Gaussian trap, the signal on the QPD would be perfectly symmetrical, and no spinning motion would be captured. The aspherical component spins with the particle and is sampled in the diagonal ratio (at twice the rotation frequency of the particle, analogous to a torch projecting light from the spinning particle onto the QPD detector plane).

Conversely, if the motion of the particle is purely orbital around the center of the trap with a fixed orientation of the asymmetry (*i.e.*, no spinning) both the transverse and the diagonal ratios exhibit a spectral peak at the orbiting frequency f_o as shown in Figure 2b. This is because any excess (asymmetrical) intensity will always have the same orientation. This asymmetry is manifested as a slight bias in one of the transverse ratios. The slight bias is seen in Figure 2b where the L/R transverse ratio has a slightly negative mean value while the diagonal ratio is effectively zero regardless of the particle position. The PSD of an orbiting, nonrotating sphere is given in Figure 2f where f_o = 1 kHz and results in a spectral peak at f_o in both the diagonal and the transverse ratio signals. A perfectly spherical particle (*i.e.*, one where $g(\theta, \phi) = 1$, would still give results similar to those shown in the figure because the orbiting frequencies captured by the QPD are due to motion of the particle itself relative to the center of the trap and not to the asymmetry of spinning around the center of the particle. In the "torch" analogy described above for an asymmetric particle, the position of the asperity (*i.e.*, torch) is fixed in the same orientation compared to the center of mass of the particle, and the scattered light from it does not contribute to the rotational motion sensed by the QPD. *It is interesting to note that observation of the spectral frequencies obtained from the transverse ratio versus those obtained from the diagonal ratio allow describing whether the motion of the particle is spinning or orbital, or a combination of both.*

Further insight can be gained by simulating the stochastic motion of a particle confined to a LP or CP Gaussian trap. To simulate the motion of the nanoparticle, we solve the translational and rotational Langevin equation of motion. At every time step in the simulation, the electrodynamic force and torque on the spheroidal nanoparticle due to the Gaussian trap is solved for using the T-matrix method;[43] see the Supporting Information for more details. Figure 2c,g shows the time trajectories and the PSD of a particle confined in an LP Gaussian trap with an incident power of 50 mW and a fwhm of 1080 nm. The particle is subject to Brownian rotational and translational fluctuations. As can be seen, no peak arises in any of the measured spectra, and the PSD plots of the simulated diagonal and transverse ratios agree with the experimental results shown in Figure 1b.

When the simulated particle is placed in a CP trap under the incident power and focusing trapping conditions an orientational force arises and driven rotational motion becomes part of the Langevin equation. Therefore, we observe the emergence of peaks in the transverse and diagonal ratios corresponding to spinning motion of the particle around its axis at a frequency of $f_s \approx 3.3$ kHz (Figure 2d,h). The peak in the transverse ratios is observed at f_s, while the diagonal ratio yields a peak at $f_c = 2f_s \approx 6.7$ kHz. The peak is wider than for the previous simulated trajectories (namely, pure spin and pure orbit cases shown in Figure 2a,b) because of Brownian rotational fluctuations of the particle. The spinning frequency of the particle is not fixed but depends on the amount of light it absorbs and scatters. Therefore, its instantaneous rotational velocity depends on the particle's distance from the center of the trap. The resultant broader spectral peak is therefore a better approximation of the experimental results than the peaks obtained from the deterministic trajectories simulated in Figure 2b,d.

The Brownian motion simulated in Figures 2d is obtained by rigorously solving the rotational and translational Langevin equation, which satisfies the fluctuation dissipation theorem and takes into account the anisotropy of the friction and Brownian noise (*i.e.*, the Brownian fluctuations are different along the long axis of the particle compared to the short axis). The GMT-Langevin dynamics simulation rigorously captures that thermal (Gaussian-white) noise on the particle position and rotation and viscous drag (friction) of an actual Ag or Au nanoparticle in water solution as well as the electrodynamic forces that act on these particles.[44,45] The simulations also take into account spin−orbit coupling and hydrodynamic effects[46] (see the Supporting Information for additional information). In less stiff optical traps where the particle is less confined to the center of the trap, we expect to see additional noise in the diagonal ratio temporal signal.

To be clear, the simulations presented in Figure 2 are of two types. Panels a and b and their respective PSDs (shown in panels e and f) represent simulations of deterministic motion of the particle undergoing pure spinning (panel a) or pure orbital (panel b) motion. These simulations were run with a time step of 0.16 ms and a total of 10^5 steps (simulated time was 1.6 s). The results shown in panels c and d represent simulations of an optically trapped particle manifesting hydrodynamic and electrodynamic forces as well as Brownian fluctuations. The particle position and orientation were sampled at a frequency of 100 MHz, and the simulation was run for 1 M steps (the simulated duration was 10 ms, which was sufficient to observe the rotation effects). We ran 28 simulations for particles with different AR values under different trapping powers.

EXPERIMENTAL DEPENDENCE ON PARTICLE SIZE

We conducted experiments in which we trapped a single Ag nanoparticle (particle diameter was 150 nm) in a CP Gaussian trap at different incident powers (Figure 3). Figure 3a,b shows the normalized PSDs of the diagonal and transverse ratios of the QPD voltage. As has been shown in the past,[3,4] increasing the laser intensity results in an increase in the particle spinning frequency. However, while the diagonal ratio allows observing the particle spinning even at low powers (*e.g.*, the P_{in} = 4 mW curve in Figure 3a), the analogous peak is not visible in the

https://doi.org/10.1021/acsphotonics.1c00802
ACS Photonics 2021, 8, 3162−3172

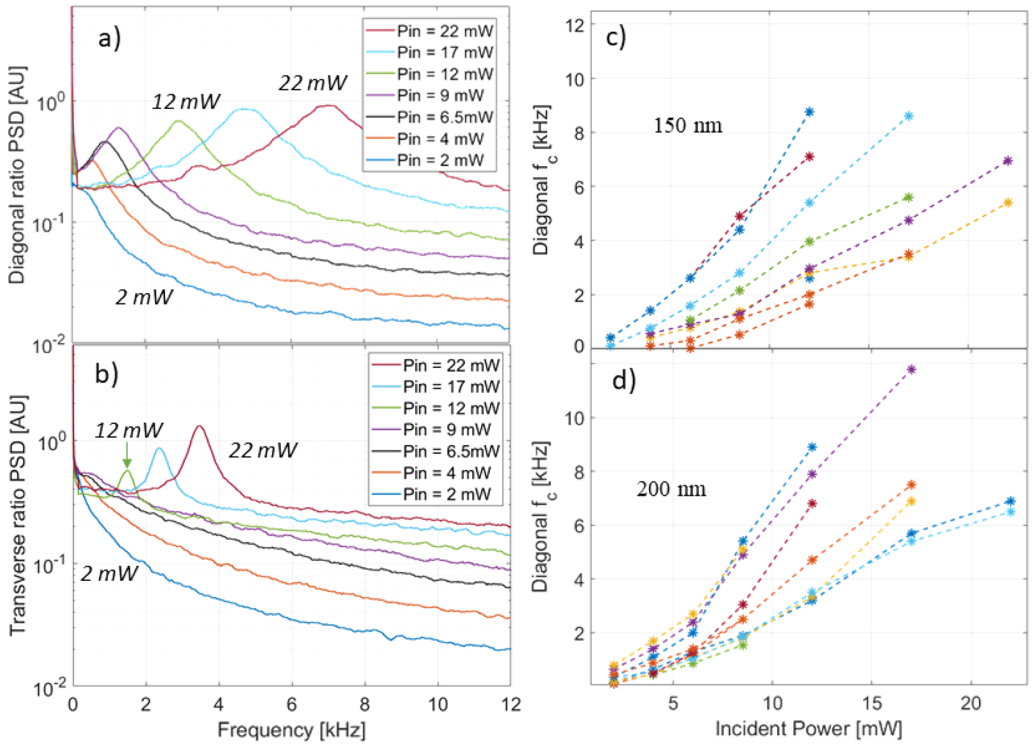

Figure 3. Experimental results from trapping a single 150 nm Ag nanoparticle in a circularly polarized Gaussian trap with varying trapping powers. (a) Measured diagonal QPD voltage ratio. Note the increase in frequency of the peak f_c as a function of power. This peak corresponds to $2f_s$. The spike in the PSDs at very low (*i.e.*, near zero) frequencies is due to the baseline DC voltage. (b) Simultaneously measured L/R transverse QPD voltage ratio (U/D ratio exhibits similar behavior). Note the emergence of a peak at higher trapping laser powers that corresponds to the spinning frequency f_s. Data shown in the PSD plots were smoothed with a rolling filter for clarity (see the Supporting Information for an example). Peak positions were determined by fitting a Lorentzian function to the raw data (c and d) (curve fitting was done on unfiltered data; see the Supporting Information for explanation). Measured peak frequency of the diagonal voltage as a function of incident power for (c) 150 nm diameter nanoparticles and (d) 200 nm diameter nanoparticles. Note the increase in spinning frequency with the incident power and variability in measured value of f_s for different particles at a given trapping power (in general agreement with previously reported results[3,4]). Note that each color in panels c and d represents a different trapped particle.

transverse ratios. This is because the background noise level at lower frequencies is larger for the transverse measurements (see Figure 1). We can only observe a peak in the transverse ratio associated with particle spinning at a higher incident power (P_{in} = 12 mW in Figure 3b). As a result, the diagonal ratio measurement we are introducing in this paper allows measuring rotational dynamics of a particle at much lower incident optical power densities than the transverse ratio. The increase in sensitivity can be seen from analyzing the results from multiple experiments on single 150 nm Ag nanoparticles (Figure 3c). We observe rotational motion at frequencies even below 200 Hz, compared to a sensitivity threshold of more than 1 kHz for the transverse ratio measurement (*e.g.*, see ref 4 and representative example in Figure 3b); a 5-fold sensitivity enhancement is measured for the identical nanoparticles in the comparisons (see the Supporting Information for further analysis).

We repeated the experiment by trapping Ag particles of nominally 150 and 200 nm diameters as specified by the manufacturer (Nanocomposix; polyvinylpyrrolidone; PVP-coated) and analyzing the measured frequencies f_c ($f_c = 2f_s$ for pure spinning) as a function of incident laser power. Representative results are shown in Figure 3c,d. In all cases, the spinning frequency increased monotonically with the incident power (the apparent superlinear increase in particle spinning frequency and its causes are addressed in the following section about evolution of particle dynamics). The distribution of spinning frequencies of the particles for a given power is due to the different aspect ratios (and sizes) of the particles, which are not perfectly spherical. Indeed, a perfectly spherical particle would not give any signal of spinning motion in the diagonal or transverse ratio measurements (see the Supporting Information for FDTD simulations of the light scattered from an asymmetric particle). An additional cause of the distribution of spinning frequencies is that the particles are coated with varying thickness of ligands, resulting in a variation of the rotational friction. Furthermore, different particle geometries and the electrostatic charge of the ligands create differences in the distance between the particles and the electrostatically charged coverslip, which leads to an additional power-dependent change in the rotational drag.[47] At higher trapping powers, thermal effects also need to be taken into account,[36] and differences in the particle shape and ligand distribution cause additional differences between the spinning frequency of different particles. Our results are consistent with previous experiments on single spinning particles.[4]

EFFECT OF ASPECT RATIO ON ROTATIONAL PARTICLE DYNAMICS OF A SPINNING SPHEROID

To better understand the variability in spinning frequencies of nanoparticles of the same type (*i.e.*, the 150 nm diameter Ag NPs observed in Figure 3c) under identical trapping conditions, we performed simulations of the expected dynamics and QPD response for particles with varying aspect

https://doi.org/10.1021/acsphotonics.1c00802
ACS Photonics 2021, 8, 3162−3172

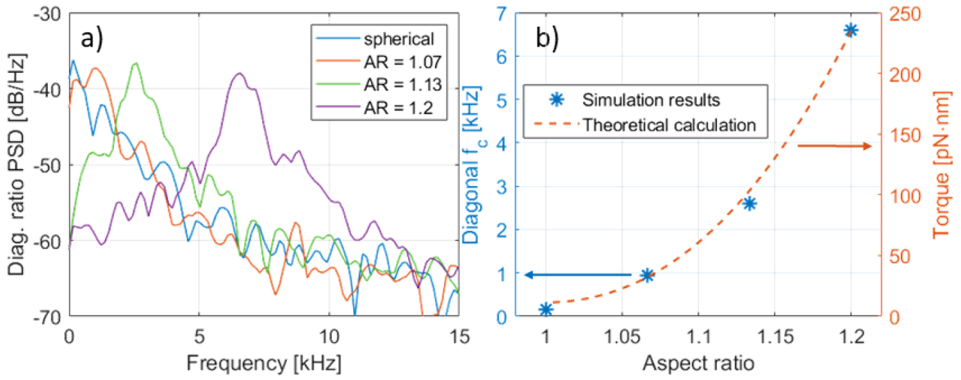

Figure 4. Calculated and simulated dependence of the spinning frequency of a spheroidal NP on its AR. (a) Simulated PSDs of the diagonal QPD ratios of prolate Ag nanoparticles with a fixed volume and an effective radius of 75 nm. We simulated the dynamics of the NPs and used the resultant trajectories to simulate the effective QPD response. (b) Fitted peaks of the PSD of the diagonal ratio (blue stars) and calculated torque (for dashed curve and RHS scale) acting on a prolate Ag nanoparticle with different aspect ratios (see text). Simulations were done using a Gaussian trap with width w_0 = 1200 nm and power P = 28 mW at a temperature T = 300 K.

ratios (ARs). We considered a spheroidal nanoparticle with minor radius a and major radius b, and defined the equivalent radius as $r_{eq} = (a^2b)^{1/3}$ (full details are provided in the Supporting Information). The equivalent radius is the radius of a sphere that can be deformed into the spheroid, preserving its volume. The aspect ratio of the simulated sphere was defined as = b/a. When $\delta > 1$, the spheroid is prolate, and when $\delta < 1$, the particle is oblate. We simulated the motion of prolate Ag nanospheres with a fixed volume; an effective radius of 75 nm; and ARs of 1, 1.07, 1.13, and 1.2. The AR range from 1 to 1.2 is in accordance with the measured AR values ascertained from TEM images of the nanoparticles (see the Supporting Information for more details). We calculated the PSD of the diagonal ratio using the same method described in Figure 2g,h. The results of the PSD calculations are shown in Figure 4a; the spinning frequency increases with the AR.

We determined the electrodynamic torque acting on the nanoparticle using T-matrix theory and the Maxwell stress tensor. The torque was calculated on nanoparticles with ARs between 1 and 1.2, where the long axis of the particle was set along the x-axis (corresponding to rotation about the z-axis). The results of the torque calculation are shown in Figure 4b (tan dashed curve) along with fitted spectral peaks from the simulations shown in Figure 4a (blue stars). The calculated torque and the simulated spinning frequencies are in excellent agreement.

These results demonstrate the importance of the particle aspect ratio in determining the observed spinning dynamics. An increase of the AR of a nanoparticle directly increases the torque applied to it. However, an increased torque also causes an increase in the viscous rotational drag on the particle. As a result, the size and AR of the particle contribute nontrivially to the particle motion. We theoretically explore the dependence between the particle's AR and the motion it exhibits in the Supporting Information. For particles that are slightly anisotropic (AR < 1.2), analytic expressions are obtained for the average angular velocity and rotational diffusion coefficient of the rotating spheroid. Overall, small deviations of the nanoparticle aspect ratio can result in substantial variations of the measured rate of spinning.

EVOLUTION OF PARTICLE DYNAMICS

Figure 5a shows the diagonal ratio and diagonal frequency measured for a 150 nm Ag nanoparticle trapped in a high-power Gaussian trap (P_{in} = 17 mW). The data shown were acquired after the particle was trapped at high power for 5 min. In the last few seconds of the trajectory we observed a gradual increase in the spinning frequency of the particle (seen as the red connected marks in Figure 5a). After 3.6 s from the start of the displayed data, the particle is deposited (or optically "printed") onto the coverslip.[37,48] From that point on, the particle is immobile and the measured voltage values remain constant along with the corresponding ratios.

To verify that the increased spinning frequency is a result of a persistent change to the particle, we performed the experiment described in Figure 5b, in which a single 150 nm PVP-coated Ag nanoparticle was trapped at a sequence of different optical powers. At a high power (P_{in} = 14 mW, blue connected dots), we observed a gradual increase in the spinning frequency. We then reduced the optical power (P_{in} = 6.5 mW, red connected dots). If the increased spinning frequency is due solely to particle heating, then a decrease in the optical power should allow the particle to cool, and the spinning frequency should revert to its original rate. However, as can be seen from the experiment, the change is persistent; when the intensity was increased again (to P_{in} = 9 mW, green connected dots and to P_{in} = 14 mW) the spinning frequency was greater than before. We repeated the power reduction again and observed an additional increase in the spinning frequency (compare the low-power period at 50 s where $f_c \approx 4$ kHz to the low-power period at 125 s where $f_c \approx 7$ kHz). The increase is monotonic. At the end of the experiment (after roughly 220 s), the particle became stuck to the electrostatically charged coverslip.

We accurately tracked the frequency increase of the particle *in situ* and in real time using the diagonal ratio of the QPD. We observed similar irreversible power-dependent behavior for other single nanoparticles in analogous experiments with alternating sequences of optical trapping powers (results not shown) indicating that the progressively increasing rotational frequency occurred for 12 nanoparticles studied in this repeated power cycling manner.

The gradual increase in the spinning frequency of the particle and its sticking to the surface is caused by several factors. The first is shedding of the ligands covering the surface of the particle. As the particle is heated by the trapping laser, the PVP covering it is damaged or released to the surrounding solution (water) environment. The shedding of ligand (and/or

https://doi.org/10.1021/acsphotonics.1c00802
ACS Photonics 2021, 8, 3162−3172

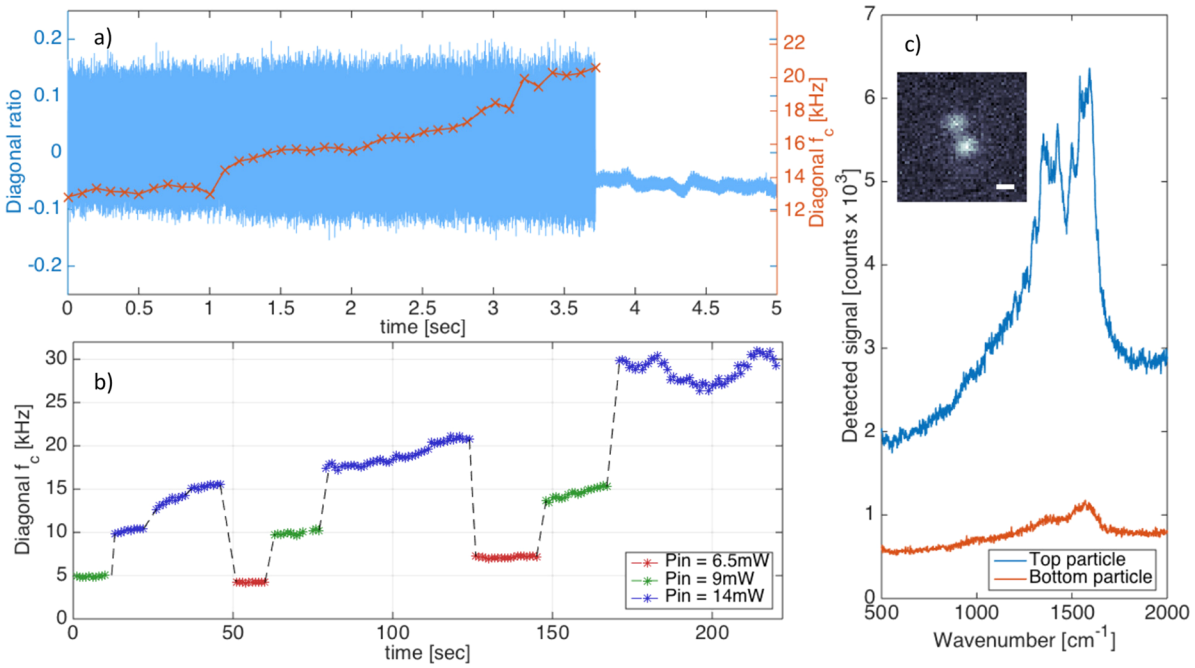

Figure 5. Analysis of changes in the frequency of single spinning nanoparticles. (a) Time trace of the diagonal ratio (blue) and moving average of the corresponding mean frequency (red) of a PVP-coated 150 nm diameter Ag nanoparticle trapped in a CP focused Gaussian trap. The measured mean frequency increases as the particle spins faster until it becomes stuck on the coverslip surface at 3.6 s. (b) Time trace of the fitted central frequency of the peak of the diagonal ratio PSD of a different single PVP-coated 150 nm Ag nanoparticle trapped in a CP Gaussian trap. Different colors designate different incident powers. Note that at higher powers we observe a monotonic increase in the fitted mean frequency of the Lorentzian, f_c, and that decreasing the optical power does not revert the spinning frequency to its original value. The trend in the frequency change is not reversible. (c) Measured Raman spectra comparing a particle that was optically trapped at a high intensity for 5 min and deposited (*i.e.*, optically printed) on the coverslip (bottom particle in the inset, red curve) and a particle that was immediately deposited on the coverslip (top particle in the inset, blue curve) without prolonged exposure to the trapping laser intensity. Raman laser wavelength is 475 nm. Inset: darkfield image of both the particles stuck on the coverslip; scale bar is 500 nm.

nanoparticle material) results in a decrease in the rotational friction coefficient[47] $\gamma_{rot}(T) = 8\pi\eta(T)r^3$, where r is the nanoparticle radius and $\eta(T)$ is the temperature-dependent viscosity of the surrounding water, which decreases at higher temperatures. Another factor is the change in the separation between the particle and the coverslip that is dictated by the Coulomb repulsion between the particle and coverslip[48] as well as the radiation pressure (scattering force) of the trapping laser.[49,50] The removal of ligands also results in a reduction in the charge on the surface of the particle, which causes the particle to move closer to the coverslip. Finally, when the charge is too low, the radiation pressure and random thermal fluctuations of the particle can overcome the repulsive electrostatic potential, causing it to be optically printed onto the coverslip and become stuck (immobile).

In order to verify the hypothesis of PVP shedding from the trapped particles, we removed the coverslip after optical trapping and after we caused several nanoparticles to become stuck after trapping and used a confocal Raman microscope with a wavelength of 473 nm (Horiba; HR evolution) to measure the signature of the molecular bonds corresponding to PVP. Figure 5c shows representative Raman spectra of two particles: the bottom spectrum (red) is of a particle that was trapped for over 5 min before being printed onto the surface, while the top spectrum (blue) is of a particle that was printed to the surface immediately after entering the optical trap. Because the rapidly immobilized particle was heated for only a few seconds, we assume this was not long enough to shed a significant portion of its ligands. The latter nanoparticle (blue spectrum) exhibits strong Raman peaks at 1426, 1490, and 1590 cm^{-1} corresponding to the signature of CH_2 vibrations, C═N stretch bend and a C═O bond stretching previously reported for PVP-coated nanoparticles.[51,52] By comparison, the long trapped and irradiated Ag nanoparticle exhibits a far weaker signal consistent with shedding of the PVP ligands caused by laser light absorption-induced heating.

We repeated the confocal Raman measurements on particles that were optically trapped for varying lengths of time and optically printed onto the coverslip. We compared particles that were trapped for long time periods (>3 min; 3 particles) to particles that were trapped for short periods of time (<3 min; 4 particles). The particles trapped for short periods of time exhibited a Raman signal that was a factor of 3 more intense than the particles trapped for long periods of time (see the Supporting Information for details).

The change in the measured Raman signal reflects the shedding of the PVP coating as a result of heating of the particle in the trap. When a nanoparticle is trapped in a laser field, it absorbs part of the incident light, resulting in a temperature increase to the particle and the fluid around it.[36,53] It has been shown that this heating leads to photothermal shedding of the ligands coating the particle.[38] The loss of PVP reduces the rotational friction acting on the particle allowing its spinning rate to increase. The QPD diagonal ratio measurement allows observing this effect in real time (see Figure 5a) for PVP-coated Ag nanoparticles.

An important effect that can occur during the trapping is deformation of the particle due to its heating.[36] A change in

https://doi.org/10.1021/acsphotonics.1c00802
ACS Photonics 2021, 8, 3162−3172

the particle shape would considerably alter the trapping dynamics and extinction cross section[54] of the particle as well as any localized surface plasmons that are excited in it. However, the particle heating and reshaping would have to increase the irregularity (*e.g.*, aspect ratio) of its shape to cause faster spinning. We suppose that to be unlikely and that heating and surface tension would make the particle shape more regular. Nevertheless, the behavoir of nonspherical particles is nontrivial[55,56] and is a subject of ongoing research.

■ ORIGIN OF THE ENHANCED SENSITIVITY OF THE DIAGONAL RATIO MEASUREMENT

The utility in using the diagonal ratio of the QPD to identify rotational motion is that it exhibits lower noise compared to the transverse ratios. Figures 1b–d and 2g,h show representative experimental and theoretical examples in which the noise level of the diagonal ratio is lower than that of the transverse ratios (*e.g.*, at low frequencies). The reason for the difference can be understood by analyzing the particle motion, the resultant ratios (transverse or diagonal), and their probability densities (see Figure 6).

The transverse ratios are direct measurements of the particle's x and y positions in the trap. In a Gaussian trap the particle positions are Gaussian distributed, and therefore, so are the transverse ratio values.[20,21] The driven spinning component of the motion contributes less to the measured voltages than the particle displacement from the center. Therefore, as shown in Figure 1, we do not observe the spinning (periodic) motion in the probability distribution in Figure 6a and only weakly in the PSD of Figure 1c. Conversely, the diagonal ratio is not sensitive to motion of the particle away from the trap center because the voltages are balanced in the x and y directions. For example, a particle moving in the $+y$ position will not increase the ratio measured in eq 2 (as it would do in eq 1b) because the increase in the top quadrants V_1 and V_2 will cancel out. This effect, similar to that seen in balanced photodetectors, means that the driven rotational motion (evident in the bimodal probability distribution seen in Figure 6b) can be readily observed in the PSD of the diagonal ratio as shown in Figure 1c.

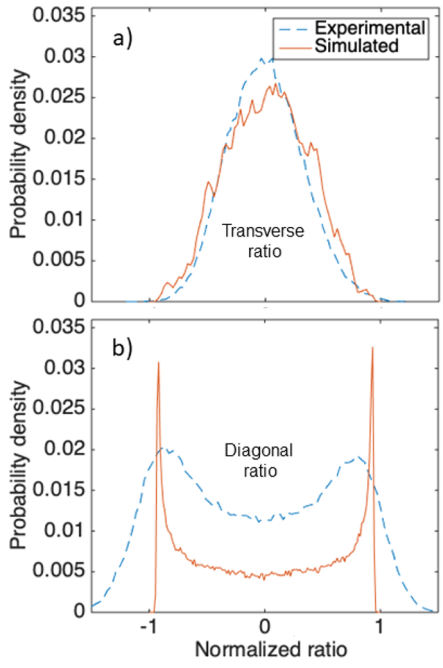

Figure 6. Distributions of the QPD signals for transverse and diagonal ratios of rotationally driven Ag nanoparticles. (a) Probability distributions for experimental (blue dashed) and simulated (red solid) values of U/D ratio. Both can be well fit to a normal distribution as expected from a thermal distribution of particle positions in a harmonic trap. (b) Probability distributions for experimental and simulated diagonal ratios. The bimodal distribution is due to the driven rotational motion of the particle, which exhibits a $\sin(2\theta)$ dependence in addition to weaker contributions from random rotation and spin–orbit coupling. The general shapes agree, but the experimental result is broader because of the irregular particle shape and scattering.

■ CONCLUSIONS

We demonstrated that the "diagonal ratio" of the QPD voltages resulting from the interference between the reflected laser beam and the light backscattered from the trapped particle is a new low-noise method for sensitive measurement of the rotational motion of only slightly anisotropic (nano-) particles in an optical trap. This method is simple and inexpensive and requires no additional equipment beyond a standard QPD of the sort that is commonly used to calibrate the particle position in an optical trap. We demonstrate a 5-fold increase in sensitivity of the diagonal ratio versus the widely used measured ratios (U/D and L/R) to detect rotational motion. The increased sensitivity of the diagonal ratio measurement even allows measuring the rotational motion of "ultra-spherical" Au nanoparticles (see the Supporting Information).

Trapping particles with 2-fold, 3-fold, or higher-order symmetrical structures should still result in a peak at $2f_s$, because the frequency doubling is enforced by the 2-fold symmetry of the diagonal ratio (V_3-V_1 vs V_4-V_2). Thus, an asymmetrical system rotating at f_s will still be sampled at $2f$. There is an interest in testing this concept theoretically and experimentally with different measurement configurations (or ratios). Such exploration could allow shape-based sorting of nanoparticles and is a topic of further research.

In the simulations and experiments described in this paper the incident light was CP, and there was no polarization dependence in the collection of the light. The polarized light scattered from the nanoparticle is not trivial to analyze and depends on the plasmonic resonance of the particle versus that of the trapping beam (see ref 44 for examples of modal decomposition of scattered light). Further research is required to understand the nature of the scattered light and adapt measurement techniques to make use of it for further motion and particle diagnosis.

Analysis of the diagonal ratio could also allow extracting useful information in cases where the rotational motion observed is of more than one particle.[3] In such cases, an analysis of the transverse and diagonal ratios could be used to ascertain information about the orientation, positions, and interparticle separation of optically bound particle pairs at high speed. This information cannot be obtained using any other contemporary angular analysis measurement method at rates well beyond video microscopy, imaging, and particle tracking analysis. Making use of the rapid information given from the QPD diagonal ratio will be crucial for fast and precise control of optically controlled nanomachines and their many applications.[44,57]

https://doi.org/10.1021/acsphotonics.1c00802
ACS Photonics 2021, 8, 3162–3172

The diagonal signal from a QPD is a simple tool that is easy to align and incorporate into an optical trapping setup and makes use of equipment that already exists in many optical trapping setups (although these specific signals are almost never extracted). We show that using the PSD of the QPD diagonal ratio enables higher sensitivity measurements than the transverse ratios because of its lower noise, thus allowing measurement of weaker signals (*e.g.*, due to smaller asymmetry of particle shape) at lower trapping powers and/or slower rates of rotation. Therefore, measuring the diagonal ratio is an inexpensive, simple, and sensitive technique that could be easily adopted by the optical trapping community. We believe that this inexpensive and readily available method will be broadly useful to researchers across scientific fields who are interested in orientational dynamics.

■ ASSOCIATED CONTENT

Supporting Information

The Supporting Information is available free of charge at https://pubs.acs.org/doi/10.1021/acsphotonics.1c00802.

Experimental and theoretical methods (PDF)

■ AUTHOR INFORMATION

Corresponding Author

Norbert F. Scherer − *James Franck Institute, The University of Chicago, Chicago, Illinois 60637, United States; Department of Chemistry, The University of Chicago, Chicago, Illinois 60637, United States;* orcid.org/0000-0002-9425-8234; Email: nfschere@uchicago.edu

Authors

Yuval Yifat − *James Franck Institute, The University of Chicago, Chicago, Illinois 60637, United States; Innoviz Technologies Ltd, Rosh Ha'Ayin 4809202, Israel;* orcid.org/0000-0003-0952-556X

John Parker − *James Franck Institute, The University of Chicago, Chicago, Illinois 60637, United States; Department of Physics, The University of Chicago, Chicago, Illinois 60637, United States;* orcid.org/0000-0001-8157-2403

Tian-Song Deng − *James Franck Institute, The University of Chicago, Chicago, Illinois 60637, United States;* Present Address: School of Electronics and Information Engineering, Hangzhou Dianzi University. No. 1158, second Avenue, Baiyang Street, Hangzhou 310018, China; orcid.org/0000-0002-0841-4932

Stephen K. Gray − *Center for Nanoscale Materials, Argonne National Laboratory, Argonne, Illinois 60439, United States*

Stuart A. Rice − *James Franck Institute, The University of Chicago, Chicago, Illinois 60637, United States; Department of Chemistry, The University of Chicago, Chicago, Illinois 60637, United States*

Complete contact information is available at: https://pubs.acs.org/10.1021/acsphotonics.1c00802

Author Contributions

N.F.S. and Y.Y. conceived of the study. Y.Y. performed the experiments and QPD simulations for this work. J.P. performed the electrodynamics−Langevin dynamics simulations to capture the trajectories of the trapped particles. T-S.D. performed the TEM characterization of the nanoparticles. S.K.G, S.A.R, and N.F.S oversaw the project. All authors contributed to writing this paper.

Notes

The authors declare no competing financial interest.

■ ACKNOWLEDGMENTS

The authors acknowledge support from the Vannevar Bush Faculty Fellowship program sponsored by the Basic Research Office of the Assistant Secretary of Defense for Research and Engineering and funded by the Office of Naval Research through Grant N00014-16-1-2502. We thank the W.M. Keck Foundation for partial support. We thank the University of Chicago Research Computing Center for an award of computer time required for the T-matrix-Langevin simulations. Electrodynamic simulations of the fields were performed at the Center for Nanoscale Materials, a U.S. Department of Energy Office of Science User Facility under Contract No. DE-AC02-06CH11357. We thank the University of Chicago NSF-MRSEC (DMR-0820054) for central facilities support. We made use of the Pritzker Nanofabrication Facility of the Institute for Molecular Engineering at the University of Chicago, which receives support from SHyNE, a node of the National Science Foundation's National Nanotechnology Coordinated Infrastructure (NSF NNCI-1542205). The authors acknowledge financial support from National Natural Science Foundation of China (NSFC, Grant No. 61905056).

■ REFERENCES

(1) Friese, M. E. J.; Nieminen, T. A.; Heckenberg, N. R.; Rubinsztein-Dunlop, H. Optical alignment and spinning of laser-trapped microscopic particles. *Nature* **1998**, *394*, 348−350.

(2) O'Neil, A. T.; MacVicar, I.; Allen, L.; Padgett, M. J. Intrinsic and extrinsic nature of the orbital angular momentum of a light beam. *Phys. Rev. Lett.* **2002**, *88*, 053601.

(3) Sule, N.; Yifat, Y.; Gray, S. K.; Scherer, N. F. Rotation and Negative Torque in Electrodynamically Bound Nanoparticle Dimers. *Nano Lett.* **2017**, *17*, 6548.

(4) Lehmuskero, A.; Ogier, R.; Gschneidtner, T.; Johansson, P.; Käll, M. Ultrafast spinning of gold nanoparticles in water using circularly polarized light. *Nano Lett.* **2013**, *13*, 3129−3134.

(5) Hajizadeh, F.; et al. Brownian fluctuations of an optically rotated nanorod. *Optica* **2017**, *4*, 746.

(6) Arita, Y.; Mazilu, M.; Dholakia, K. Laser-induced rotation and cooling of a trapped microgyroscope in vacuum. *Nat. Commun.* **2013**, *4*, 2374.

(7) La Porta, A.; Wang, M. D. Optical torque wrench: Angular trapping, rotation, and torque detection of quartz microparticles. *Phys. Rev. Lett.* **2004**, *92*, 190801.

(8) Inman, J.; Forth, S.; Wang, M. D. Passive torque wrench and angular position detection using a single-beam optical trap. *Opt. Lett.* **2010**, *35*, 2949−2951.

(9) Monteiro, F.; Ghosh, S.; Fine, A. G.; Moore, D. C. Optical levitation of 10-ng spheres with nano-g acceleration sensitivity. *Phys. Rev. A: At., Mol., Opt. Phys.* **2017**, *96*, 63841.

(10) Reimann, R.; et al. GHz Rotation of an Optically Trapped Nanoparticle in Vacuum. *Phys. Rev. Lett.* **2018**, *121*, 033602.

(11) Arita, Y.; et al. Rotational Dynamics and Heating of Trapped Nanovaterite Particles. *ACS Nano* **2016**, *10*, 11505−11510.

(12) Ashkin, A. Acceleration and trapping of particles by radiation pressure. *Phys. Rev. Lett.* **1970**, *24*, 156.

(13) Grier, D. G. A revolution in optical manipulation. *Nature* **2003**, *424*, 810−816.

(14) Neuman, K. C.; Block, S. M. Optical trapping. *Rev. Sci. Instrum.* **2004**, *75*, 2787−283.

(15) Svoboda, K.; Block, S. M. Biological applications of optical forces. *Annu. Rev. Biophys. Biomol. Struct.* **1994**, *23*, 247−285.

(16) Maragò, O. M.; et al. Optical trapping and manipulation of nanostructures. *Nat. Nanotechnol.* **2013**, *8*, 807−819.

(17) Spesyvtseva, S. E. S.; Dholakia, K. Trapping in a Material World. *ACS Photonics* **2016**, *3*, 719−736.
(18) Gittes, F.; Schmidt, C. F. Interference model for back-focal-plane displacement detection in optical tweezers. *Opt. Lett.* **1998**, *23*, 7.
(19) Pralle, A.; Prummer, M.; Florin, E. L.; Stelzer, E. H. K.; Hörber, J. K. H. Three-dimensional high-resolution particle tracking for optical tweezers by forward scattered light. *Microsc. Res. Tech.* **1999**, *44*, 378−386.
(20) Berg-Sørensen, K.; Flyvbjerg, H. Power spectrum analysis for optical tweezers. *Rev. Sci. Instrum.* **2004**, *75*, 594.
(21) Tolić-Nørrelykke, S. F.; et al. Calibration of optical tweezers with positional detection in the back focal plane. *Rev. Sci. Instrum.* **2006**, *77*, 103101.
(22) Carter, A. R.; King, G. M.; Perkins, T. T. Back-scattered detection provides atomic-scale localization precision, stability, and registration in 3D. *Opt. Express* **2007**, *15*, 13434−13445.
(23) Wang, M. D.; Yin, H.; Landick, R.; Gelles, J.; Block, S. M. Stretching DNA with optical tweezers. *Biophys. J.* **1997**, *72*, 1335−1346.
(24) Woodside, M. T.; et al. Direct measurement of the full, sequence-dependent folding landscape of a nucleic acid. *Science (Washington, DC, U. S.)* **2006**, *314*, 1001−1004.
(25) Ma, J.; Bai, L.; Wang, M. D. Transcription Under Torsion. *Science (Washington, DC, U. S.)* **2013**, *340*, 1580−1583.
(26) Liphardt, J.; Onoa, B.; Smith, S. B.; Tinoco, I.; Bustamante, C. Reversible unfolding of single RNA molecules by mechanical force. *Science (Washington, DC, U. S.)* **2001**, *292*, 733−737.
(27) Schnitzer, M. J.; Visscher, K.; Block, S. M. Force production by single kinesin motors. *Nat. Cell Biol.* **2000**, *2*, 718−723.
(28) Perkins, T. T. Optical traps for single molecule biophysics: A primer. *Laser Photonics Rev.* **2009**, *3*, 203−220.
(29) Li, T.; Kheifets, S.; Medellin, D.; Raizen, M. G. Measurement of the instantaneous velocity of a Brownian particle. *Science* **2010**, *328*, 1673−5.
(30) Pelton, M.; et al. Optical trapping and alignment of single gold nanorods by using plasmon resonances. *Opt. Lett.* **2006**, *31*, 2075−7.
(31) Yan, Z.; et al. Three-dimensional optical trapping and manipulation of single silver nanowires. *Nano Lett.* **2012**, *12*, 5155−5161.
(32) Tong, L.; Miljković, V. D.; Käll, M. Alignment, rotation, and spinning of single plasmonic nanoparticles and nanowires using polarization dependent optical forces. *Nano Lett.* **2010**, *10*, 268−273.
(33) Kuhn, S.; et al. Full rotational control of levitated silicon nanorods. *Optica* **2017**, *4*, 356.
(34) Bonin, K.; Kourmanov, B.; Walker, T. Light torque nano-control, nanomotors and nanorockers. *Opt. Express* **2002**, *10*, 984−989.
(35) Shao, L.; Käll, M. Light-Driven Rotation of Plasmonic Nanomotors. *Adv. Funct. Mater.* **2018**, *28*, 1706272.
(36) Baffou, G.; Quidant, R. Thermo-plasmonics: Using metallic nanostructures as nano-sources of heat. *Laser and Photonics Reviews* **2013**, *7*, 171−187.
(37) Bao, Y.; Yan, Z.; Scherer, N. F. Optical printing of electrodynamically coupled metallic nanoparticle arrays. *J. Phys. Chem. C* **2014**, *118*, 19315−19321.
(38) Šípová, H.; Shao, L.; Odebo Länk, N.; Andrén, D.; Käll, M. Photothermal DNA Release from Laser-Tweezed Individual Gold Nanomotors Driven by Photon Angular Momentum. *ACS Photonics* **2018**, *5*, 2168.
(39) Chen, H.; Zhao, Q.; Du, X. Light-powered micro/nanomotors. *Micromachines* **2018**, *9*, 41.
(40) Roy, B.; Bera, S. K.; Banerjee, A. Simultaneous detection of rotational and translational motion in optical tweezers by measurement of backscattered intensity. *Opt. Lett.* **2014**, *39*, 3316.
(41) Volpe, G.; Kozyreff, G.; Petrov, D. Backscattering position detection for photonic force microscopy. *J. Appl. Phys.* **2007**, *102*, 084701.
(42) Perrone, S.; Volpe, G.; Petrov, D. 10-fold detection range increase in quadrant-photodiode position sensing for photonic force microscope. *Rev. Sci. Instrum.* **2008**, *79*, 106101.
(43) Doicu, A.; Wriedt, T.; Eremin, Y. A. *Light scattering by systems of particles: null-field method with discrete sources: theory and programs*; Springer, 2006; vol. *124*.
(44) Parker, J.; et al. Optical matter machines: angular momentum conversion by collective modes in optically bound nanoparticle arrays. *Optica* **2020**, *7*, 1341−1348.
(45) Sule, N.; Rice, S. A.; Gray, S. K.; Scherer, N. F. An electrodynamics-Langevin dynamics (ED-LD) approach to simulate metal nanoparticle interactions and motion. *Opt. Express* **2015**, *23*, 29978.
(46) Ruffner, D. B.; Grier, D. G. Optical forces and torques in nonuniform beams of light. *Phys. Rev. Lett.* **2012**, *108*, 173602.
(47) Leach, J.; et al. Comparison of Faxén's correction for a microsphere translating or rotating near a surface. *Phys. Rev. E - Stat. Nonlinear, Soft Matter Phys.* **2009**, *79*, 026301.
(48) Gargiulo, J.; et al. Accuracy and Mechanistic Details of Optical Printing of Single Au and Ag Nanoparticles. *ACS Nano* **2017**, *11*, 9678.
(49) Figliozzi, P.; et al. Driven optical matter: Dynamics of electrodynamically coupled nanoparticles in an optical ring vortex. *Phys. Rev. E: Stat. Phys., Plasmas, Fluids, Relat. Interdiscip. Top.* **2017**, *95*, 022604.
(50) Han, F.; et al. Crossover from positive to negative optical torque in mesoscale optical matter. *Nat. Commun.* **2018**, *9*, 4897.
(51) Jackson, J. B.; Halas, N. J. Surface-enhanced Raman scattering on tunable plasmonic nanoparticle substrates. *Proc. Natl. Acad. Sci. U. S. A.* **2004**, *101*, 17930−17935.
(52) Moran, C. H.; Rycenga, M.; Zhang, Q.; Xia, Y. Replacement of poly(vinyl pyrrolidone) by thiols: A systematic study of Ag nanocube functionalization by surface-enhanced raman scattering. *J. Phys. Chem. C* **2011**, *115*, 21852−21857.
(53) Baffou, G.; Quidant, R.; García De Abajo, F. J. Nanoscale control of optical heating in complex plasmonic systems. *ACS Nano* **2010**, *4*, 709−716.
(54) Brzobohatý, O.; et al. Non-spherical gold nanoparticles trapped in optical tweezers: shape matters. *Opt. Express* **2015**, *23*, 8179−8189.
(55) Coursault, D.; Sule, N.; Parker, J.; Bao, Y.; Scherer, N. F. Dynamics of the optically directed assembly and disassembly of gold nanoplatelet arrays. *Nano Lett.* **2018**, *18*, 3391−3399.
(56) Brzobohatý, O.; et al. Three-dimensional optical trapping of a plasmonic nanoparticle using low numerical aperture optical tweezers. *Sci. Rep.* **2015**, *5*, 8106.
(57) Xu, L.; Mou, F.; Gong, H.; Luo, M.; Guan, J. Light-driven micro/nanomotors: from fundamentals to applications. *Chem. Soc. Rev.* **2017**, *46*, 6905−6926.

https://doi.org/10.1021/acsphotonics.1c00802
ACS Photonics 2021, 8, 3162−3172